Electronic Structure of the Neutral Tyrosine Radical in Frozen Solution. Selective ^{2}H-, ^{13}C-, and ^{17}O-Isotope Labeling and EPR Spectroscopy at 9 and 35 GHz

R. J. Hulsebosch,[†] J. S. van den Brink,[†,§] S. A. M. Nieuwenhuis,[‡] P. Gast,[†] J. Raap,[‡] J. Lugtenburg,[‡] and A. J. Hoff*[,†]

Contribution from the Department of Biophysics, Huygens Laboratory, Leiden University, P.O. Box 9504, 2300 RA Leiden, The Netherlands, and Leiden Institute of Chemistry, Gorlaeus Laboratories, Leiden University, P.O. Box 9502, 2300 RA Leiden, The Netherlands

Received January 28, 1997. Revised Manuscript Received June 4, 1997[⊗]

Abstract: Selective ^{2}H-, ^{13}C-, and ^{17}O-isotope labeling of the tyrosine amino acid has been used to map the unpaired π-electron spin-density distribution of the UV-generated neutral L-tyrosine phenoxy radical in alkaline frozen solution. The use of ^{13}C and ^{17}O labels allowed accurate determination of the full spin-density distribution and provided more insight in the geometrical structure of the neutral tyrosine radical in vitro. Simulations of the X-band (9.2 GHz) and Q-band (34.8 GHz) EPR powder spectra yielded the principal components of the ^{1}H-, ^{13}C-, and ^{17}O-hyperfine tensors. For the two β-methylene hydrogens, a static conformational distribution of the dihedral angles ($90° < \theta_1 < 60°$ and $60° < \theta_2 < 30°$) was taken into account. The major proton hyperfine interactions and the principal g values for the neutral tyrosine radical, obtained from selectively deuterated samples, are consistent with literature values. The spin density at the specifically labeled postitions (C1′, C2′, C3′, C4′, C5′, O4′) was evaluated from the anisotropy of the ^{13}C- and ^{17}O-hyperfine tensors. A quantitative analysis of the positions C3′ and C5′ provided evidence for a planar distortion of the aromatic ring at these positions. ^{17}O enrichment of the phenol oxygen O4′ of the tyrosine radical unambiguously showed that the spin density at this oxygen is 0.26 ± 0.01. From the relatively large delocalization of the spin density over the carbonyl group of the tyrosine aromatic ring system, it is concluded that the C4′−O4′ bond has a double-bond character. The experimentally determined spin-density distribution is compared with several computational calculated spin-density distributions found in the literature. The isotropic ^{13}C-hyperfine interactions are discussed in the framework of the Karplus−Fraenkel theory. This theory proved to be accurate for the determination of sign and magnitude of the isotropic ^{13}C- and ^{17}O-hyperfine interactions.

Introduction

Research during the past decade has revealed that tyrosine radicals fulfill an essential role in a number of biological processes. Tyrosine radicals have been identified in enzymes such as the ribonucleotide reductase,[1] prostaglandin H synthase,[2] and the water splitting enzyme in plant photosynthesis.[3] Possible activity of further tyrosine radicals in ribonucleotide reductase,[4] plant photosynthesis,[5,6] and other biological systems[7] has been suggested. Tyrosine-derived radicals have been identified in galactose oxidase[8] and amine oxidase.[9] For obtaining more information about the character and structure of these protein-bound radicals, comparison with the unperturbed model system, i.e., the (neutral) π-radical without protein environment, is essential. By probing the hyperfine interactions (hfi's) of the unpaired electron with a particular nucleus with $I \neq 0$, electron paramagnetic resonance (EPR) spectroscopy is a powerful tool for a detailed study of the electronic and nuclear structure of the in vitro tyrosine radical. From the obtained hfi, the spin-density distribution of the unpaired π-electron can be mapped. Both the observed hfi and the spin-density distribution of the unpaired electron are suitable probes of protein-induced structural changes, providing for example information on much debated issues as the phenoxyl oxygen−carbon bond length,[10−12] puckering of the phenoxyl ring,[10,12] and the orientation of the methylene β-protons.[13−15] A variety of EPR methods have therefore been employed: X-band EPR measurements on X-ray irradiated single crystals,[16,17] X-band electron spin−echo envelope modulation (ESEEM),[18] and

[†] Department of Biophysics.
[‡] Leiden Institute of Chemistry.
[§] Present address: Philips Medical Systems NL B.V., Magnetic Resonance Imaging, Methods Department, P.O. Box 10000, 5680 DA Best, The Netherlands.
* Corresponding author. Telephone: +31-71-5275955. FAX: +31-71-5275819. E-mail: HOFF@RULHL1.LeidenUniv.NL.
[⊗] Abstract published in *Advance ACS Abstracts,* August 1, 1997.

(1) Reichard, P.; Ehrenberg, A. *Science* **1983**, *221*, 514−519.
(2) Karthein, R.; Dietz, R.; Nastainczyk, W.; Ruf, H. H. *Eur. J. Biochem.* **1988**, *171*, 313−320.
(3) Barry, B. A.; Babcock, G. T. *Proc. Natl. Acad. Sci. U.S.A.* **1987**, *84*, 7099−7103.
(4) Allard, P.; Barra, A. L.; Anderson, K. K.; Schmidt, P. P.; Atta, M.; Gräslund, A. *J. Am. Chem. Soc.* **1996**, *118*, 895−896.
(5) Boerner, R. J.; Bixby, K. A.; Nguyen, A. P.; Noren, G. H.; Debus, R. J.; Barry, B. A. *J. Biol. Chem.* **1993**, *268*, 1817−1823.
(6) Boerner, R. J.; Barry, B. A. *J. Biol. Chem.* **1994**, *269*, 134−137.
(7) Ivancich, A.; Jouve, H. M.; Gaillard, J. *J. Am. Chem. Soc.* **1996**, *118*, 12852−12853.
(8) Whittaker, M. M.; Whittaker, J. W. *J. Biol. Chem.* **1990**, *265*, 9610−9613.
(9) Jones, S. M.; Mu, D.; Wemmes, D.; Smith, A. J.; Kaus, S.; Maltby, D.; Burlingame, A. L.; Kinman, J. R. *Science* **1990**, *248*, 981−987.
(10) Chipman, D. M.; Liu, R.; Zhou, X.; Pulay, P. *J. Chem. Phys.* **1994**, *100*, 5023−5035.
(11) Armstrong, D. R.; Cameron, C.; Nonhebel, D. C.; Perkins, P. G. *J. Chem. Soc., Perkin Trans. 2* **1983**, 569−573.
(12) Shinagawa, Y.; Shinagawa, Y. *J. Am. Chem. Soc.* **1978**, *100*, 67−72.
(13) Tommos, C.; Tang, X.-S.; Warncke, K.; Hoganson, C. W.; Styring, S.; McCracken, J.; Diner, B. A.; Babcock, G. T. *J. Am. Chem. Soc.* **1995**, *117*, 10325−10335.
(14) Warncke, K.; Babcock, G. T.; McCracken, J. *J. Chem. Phys.* **1996**, *100*, 4654−4661.
(15) Qin, Y.; Wheeler, R. A. *J. Am. Chem. Soc.* **1995**, *117*, 6083−6092.
(16) Fasanella, E. L.; Gordy, W. *Proc. Natl. Acad. Sci. U.S.A.* **1969**, *62*, 299−304.

S0002-7863(97)00787-7 CCC: $14.00

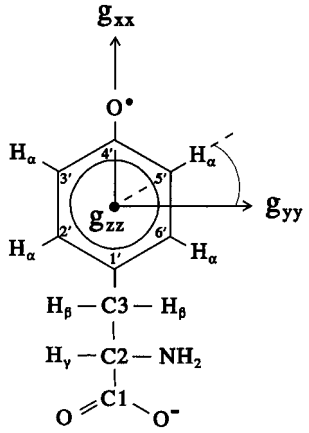

Figure 1. Numbering scheme and directions of the principal axes of the *g* matrix in the tyrosine radical. The Euler angle ϕ represents an in-plane rotation of the hyperfine components, defined in the molecular axes system, to the *g* axes frame. ϕ is positive for a clockwise rotation.

EPR[19,20] measurements on UV-illuminated, selectively deuterated tyrosines in frozen alkaline solution, and room temperature X-band EPR experiments on chemically or photooxidized tyrosine.[21,22] A number of in vitro tyrosine radical proton and deuteron hfi's were determined, and the resulting approximate spin-density distribution followed the odd-alternate pattern as was expected on theoretical grounds,[23] i.e., high spin density at the phenol oxygen O4′ and the aromatic ring carbon positions C1′, C3′, and C5′ and low spin density at the other positions (see Figure 1 for the chemical structure and nomenclature of the neutral tyrosine radical). A quantitative analysis of ESEEM spectra of in vitro ^{2}H-labeled neutral tyrosine radicals at low temperature provided evidence for a static conformational dispersion of the β-methylene protons.[14,24] None of the previous papers, however, give a full characterization of the neutral tyrosine radical in vitro. The exact spin density at the carbon position C1′ remains unclear, partially because of the disordered orientation of the methylene β-protons, the spin densities at C4′ and O4′ are not very well determined, and the sign of the spin density at C2′ and C6′ is uncertain.

As part of a program to investigate the electronic structure and binding of functionally active tyrosine radicals in vivo, we have employed EPR in combination with site-selective isotope labeling to conclusively characterize the neutral tyrosine radical in vitro. We present EPR studies at *two* different frequencies, 9.2 GHz (X-band) and 34.8 GHz (Q-band), of selectively ^{2}H-, ^{13}C-, and ^{17}O-labeled tyrosine radicals generated by UV irradiation in frozen alkaline solution. In comparison to spectra recorded at X-band, the Q-band spectra show additional structure due to the increased influence of *g*-factor anisotropy. The availability of an extra set of Q-band spectra considerably decreased the parameter range of the principle hyperfine tensor elements used for the spectral simulations. The Q-band spectrum of fully deuterated tyrosine radicals enabled us to acquire accurate values for the principal *g* values. Each individual proton hfi was assessed using selective ^{1}H/^{2}H exchange. This replacement was also helpful for fixing the ^{13}C- and ^{17}O-hfi tensors. The use of selective ^{13}C-labeling has several important advantages with respect to ^{1}H/^{2}H exchange methods. First of all, the ^{13}C-hfi tensor often directly reflects the magnitude of the spin density at the labeled carbon and is more sensitive to the geometry of the C−C, C−H, and C−O bonds than the more commonly measured proton hfi tensors, since the unpaired electron resides in an atomic orbital of the ^{13}C nucleus ($I = {}^1/_2$). Furthermore, ^{13}C-labeling probes the spin density at so-called "blind" positions where adjacent protons are absent. Finally, the hyperfine interaction with the ^{17}O isotope ($I = {}^5/_2$) provides direct information about the spin density at the tyrosine radical phenol oxygen. Note that there is no ^{13}C- or ^{17}O-isotope effect on the spin-density distribution in the π-radical.[25,26] The expected small changes of the α-proton hfi upon deuteration of the β-methylene hydrogens were ignored.[27]

A consistent set of principal hfi tensor elements for all protons, carbons, and the oxygen was obtained by simulating the spectra of a great variety of different isotope-labeled tyrosine radicals, recorded at two EPR frequencies. Incorporation of a static conformational distribution of the methylene β-protons resulted in much better simulations of the measured spectra. The accurate spin-density distribution obtained from hfi tensors giving insight in the geometrical structure of the tyrosine radical was obtained from the acquired anisotropic ^{13}C- and ^{17}O-isotope hfi. Evidence is found for a small in-plane distortion of the aromatic ring structure at the C3′ and C5′ positions. The relatively large delocalization of spin density over the carbonyl group of the tyrosine ring indicates that the C4′−O4′ bond has a predominant double-bond character.

Materials and Methods

^{2}H-, ^{13}C-, and ^{17}O-Labeling. L-Tyrosine [L-3-(4-hydroxyphenyl)-alanine] and its perdeuterated isomer, [$^2H_7$]tyrosine, were purchased from Sigma and C/D/N Isotopes Canada, respectively. Proton/deuteron exchange of the 3′ and 5′ positions of tyrosine was performed as described.[28] Specific deuteration of both β-protons and the single γ-proton was enzymatically prepared from deuterated serine in D_2O and phenol, resulting in the [2,3,3-$^2H_3$]tyrosine species.[29] ^{13}C-labeled tyrosines were synthesized as described,[29] to obtain selectively enriched singly labeled molecules with labels at the ring positions 1′, 2′, 3′, and 4′ and the doubly labeled 3′,5′ molecule (see Figure 1 for numbering scheme). NMR spectra of the labeled compounds showed that the ^{2}H and ^{13}C enrichment was better than 98%. ^{17}O-labeled tyrosine was synthesized with a 43% enrichment of the phenoxyl oxygen.[29] Several ^{13}C- and ^{17}O-labeled tyrosines were also selectively deuterated at positions 3′ and 5′. The following labeled tyrosines were thus prepared: [3′,5′-$^2H_2$]-L-tyrosine, [2,3,3-$^2H_3$]-L-tyrosine, [1′-$^{13}C_1$]-L-tyrosine, [1′-$^{13}C_1$,3′,5′-$^2H_2$]-L-tyrosine, [2′-$^{13}C_1$]-L-tyrosine, [2′-$^{13}C_1$,3′,5′-$^2H_2$]-L-tyrosine, [3′-$^{13}C_1$]-L-tyrosine, [3′-$^{13}C_1$,3′,5′-$^2H_2$]-L-tyrosine, [3′,5′-$^{13}C_2$]-L-tyrosine, [3′,5′-$^{13}C_2$,3′,5′-$^2H_2$]-L-tyrosine, [4′-$^{13}C_1$]-L-tyrosine, [4′-$^{13}C_1$,3′,5′-$^2H_2$]-L-tyrosine, and [4′-$^{17}O_1$,3′,5′-$^2H_2$]-L-tyrosine.

Sample Preparation. A 5 mM solution of a specific tyrosine was prepared in alkaline (pH 11) NaOH/H_2O to obtain deprotonation of the tyrosine. The solution was loaded into an EPR quartz sample tube and was deoxygenated by bubbling with argon for about 5 min. The tube was sealed with a rubber stopper under argon pressure and was

(17) Box, H. C.; Budzinski, E. E.; Freund, H. G. *J. Chem. Phys.* **1974**, *61*, 2222−2226.
(18) Warncke, K.; McCracken, J. *J. Chem. Phys.* **1994**, *101*, 1832−1841.
(19) Barry, B. A.; El-Deeb, M. K.; Sandusky, P. O.; Babcock, G. T. *J. Biol. Chem.* **1990**, *265*, 20139−20143.
(20) Hoganson, C. W.; Babcock, G. T. *Biochemistry* **1992**, *31*, 11874−11880.
(21) Sealy, R. C.; Harman, L.; West, P. R.; Mason, R. P. *J. Am. Chem. Soc.* **1985**, *107*, 3401−3406.
(22) Tomkiewicz, M.; McAlpine, R. D.; Cocivera, M. *Can. J. Chem.* **1972**, *50*, 3849−3856.
(23) Salem, L. *Molecular Orbital Theory of Conjugated Systems*; W. A. Benjamin, Inc.: New York, 1966.
(24) Warncke, K.; McCracken, J. *J. Chem. Phys.* **1995**, *103*, 6829−6840.
(25) McConnell, H. M.; Giuliano, C. R. *J. Chem. Phys.* **1961**, *35*, 1910−1911.
(26) Venkataraman, B.; Fraenkel, G. K. *J. Chem. Phys.* **1956**, *24*, 737−740.
(27) Stevenson, C. D.; Wagner II, E. P.; Reiter, R. C. *J. Phys. Chem.* **1993**, *97*, 10585−10588.
(28) Mathews, R. H.; Matthews, K. S.; Opella, S. J. *Biochim. Biophys. Acta* **1977**, *497*, 1−13.
(29) Winkel, C.; Aarts, M. W. M. M.; Van der Heide, F. R.; Buitenhuis, E. G.; Lugtenburg, J. *Recl. Trav. Chim. Pays-Bas* **1989**, *108*, 139−146.

slowly frozen by placing the EPR tube in a flow cryostat. For complete degassing, the samples were repeatedly thawed and refrozen. The stable neutral tyrosine radical was created by irradiation of the sample for 2 min with the full spectrum (275−335 nm) of a 100 W Oriel Mercury lamp, at 77 K. After illumination, the samples were either directly used or were stored in liquid nitrogen. No degradation of the radical signal due to storage was observed over a period of 2 months. The EPR spectrum of unlabeled tyrosine radicals generated in pH 2 H_2SO_4/H_2O closely resembled the spectrum for alkaline frozen solution (not shown). The slight differences that where observed presumably relate to small changes of the methylene β-proton hfi caused by the different protonation state of the amino ($pK_a = 9.1$[30]) and carboxyl ($pK_a = 2.2$[30]) groups of the amino acid side chain. The low solubility of tyrosine at intermediate pH values (pH 5−7) made it impossible to record a proper EPR spectrum. No qualitative changes in the EPR spectra of the all-^{1}H tyrosine were observed upon varying the pH of the NaOH solution between 8 and 13. EPR spectra of tyrosine radicals generated in alkaline NaOD (99% D, pD 11)/D_2O (99.9% D) were identical, except for some line narrowing, presumably because spin−spin relaxation induced by matrix deuterons is slower than for protonated solvents.

EPR Measurements. X-band EPR spectra were obtained using a Varian E-9 spectrometer operating at 9.2 GHz, with 100 kHz field modulation. The spectrometer was equipped with a multipurpose TE-102 cavity and a liquid nitrogen cooled gas-flow cryostat. The X-band measurements were performed at about 90 K. Q-band (34.8 GHz) EPR spectra were obtained using a home-built super-heterodyne spectrometer with low-frequency field modulation.[31] All Q-band measurements were performed in a home-built bath cryostat filled with cold N_2 gas ($T \approx$ 100 K). Low microwave powers (50 μW and 50 nW for X- and Q-band, respectively) were used in all EPR experiments to prevent saturation of the signal and attendant line broadening. X-band measurements between 20 and 100 K, using an Oxford helium flow cryostat, showed no changes in the observed spectra. We can therefore exclude dynamical activities and changes in hybridization or in the geometrical structure of the tyrosine radical that could influence the line width and shape of the EPR spectra upon changing the temperature.[32]

Simulations. Spectral simulations were obtained using a powder-EPR simulation program similar to that of Hoganson and Babcock,[20] which takes into account the appropriate nuclear g values for ^{1}H, ^{2}H, ^{13}C, and ^{17}O,[33] anisotropic hfi's and g values for up to eight nuclei, Euler angles, and a spin packet line width parameter. For the tyrosine radicals not deuterated at positions 3′ and 5′, best results were obtained with a spin packet line width parameter of about 0.26 mT, while for the 3′ and 5′ deuterated species, a value of about 0.36 mT was used. The X-band EPR spectrum of the [4′-$^{17}O_1$,3′,5′-$^2H_2$]tyrosine radical was simulated with a spin packet line width of 0.52 mT. These variations in spin packet line widths may be rationalized by a nuclear spin-dependent line broadening caused by a different relaxation behavior of the different nuclei.[34−36] The program also included a static conformational distribution of the dihedral angles of the β-methylene protons with the angle between both β-protons set to 120° (ideal sp^3 hybridization). For each conformation, the hfi tensors of both β-protons were calculated using eqs 3 and 4 with a fixed spin density of 0.32 at C1′. This spin-density value was acquired from our experiments on 1′-^{13}C-labeled tyrosines. A final simulation of an EPR spectrum consists of an average of spectra calculated for each dihedral angle conformation within certain boundaries ($90° < \theta_1 < 60°$ and $60° < \theta_2 < 30°$), with each of the conformations having the same weighting factor.[24]

Because there is considerable variety in the numerical parameter values in the literature, a brief synopsis of the relations between hfi and spin densities is given to justify the parameter values that were used in the calculations. Throughout the analysis, the overruling principle was consistency of all hfi tensor elements for the complete set of EPR spectra.

Relations among ^{1}H-, ^{2}H-, ^{13}C-, and ^{17}O-Hyperfine Interactions and Spin Densities

^{1}H-Hyperfine Interactions. Proton hyperfine interactions consist of an isotropic contribution proportional to the electron spin density at the nucleus and an anisotropic term due to the direct dipolar coupling. The relationship between the isotropic hyperfine splitting constant A_C^H for an α-proton bound to a planar π-radical, and the unpaired π-electron spin density ρ_C^π at an adjacent sp^2-hybridized carbon atom C is given by the McConnell relation[37,38]

$$A_C^{H_\alpha} = Q_{CH}^H \rho_C^\pi \tag{1}$$

The proportionality constant Q_{CH}^H is related to the $\sigma-\pi$ electron interaction. The notation used (Q_{BC}^A) is as follows: superscript (A) indicates the nucleus under consideration and the subscript (BC) the bond involved, with the first letter (B) designating the atom on which the electron is located. Empirically, Q_{CH}^H has been shown to be almost constant with values between −2 and −3 mT, the variations arising from different electric charges on the molecule. The absolute Q_{CH}^H values for positive ions tend to be larger than those for negative ions.[39] Analysis of the principal proton hyperfine tensor components for the tyrosine radical in ribonucleotide reductase from *Escherichia coli* resulted in a Q_{CH}^H of −2.49 mT.[40]

Hyperfine interactions from β-protons (protons not directly bound to the aromatic ring system) are generally of the same order of magnitude as those from α-protons and are explained by a hyperconjugation mechanism in which partial electron transfer from the β-hydrogen atoms to the p orbital of the aromatic ring carbon gives rise to unpaired spin density in the 1s orbitals of the β-hydrogen atoms. The spin density at the nucleus of the β-proton depends on the overlap between the 1s orbital of the proton and the $2p_z$ orbital of the carbon and therefore on the so-called dihedral angle θ between the $2p_z$ orbital and the plane containing the C1′−C3−H3 bonds. The total principal β-proton hyperfine tensor is given by

$$\mathbf{A}_C^{H_\beta}(\text{total}) = A_C^{H_\beta} + \mathbf{D}_C^{H_\beta} \tag{2}$$

where the isotropic hyperfine interaction, $A_C^{H_\beta}$, is semiempirically related to the spin density in the $2p_z$ orbital:[37,41]

$$A_C^{H_\beta} = B_0 \rho_{C1'}^\pi + B_1 \rho_{C1'}^\pi \cos^2\theta \tag{3}$$

The constant B_0 includes contributions from spin density that arise from conformation-independent mechanisms, in particular spin polarization, while B_1 accounts for the hyperconjugation contribution. Generally, B_0 is considered to be small and is neglected, whereas for B_1, a value of 5.8 mT has been given.[42]

(30) Dean, J. A. *Lange's Handbook of Chemistry*, 12th ed.; McGraw-Hill: New York, 1979; pp 5−41.
(31) Van den Brink, J. S.; Spoyalov, A. P.; Gast, P.; Van Liemt, W. B. S.; Raap, J.; Lugtenburg, J.; Hoff, A. J. *FEBS Lett.* **1994**, *353*, 273−276.
(32) Van den Hoek, W. J.; Huysmans, W. G. B.; Van Gemert, M. J. C. *J. Magn. Res.* **1970**, *3*, 137−145.
(33) Weil, J. A.; Bolton, J. R.; Wertz, J. E. *Eletron Paramagnetic Resonance*; John Wiley & Sons Inc.: New York, 1994.
(34) De Boer, E.; Mackor, E. L. *J. Chem. Phys.* **1963**, *38*, 1450−1452.
(35) Hudson, A.; Luckhurst, G. R. *Chem. Rev.* **1969**, *69*, 191−225.
(36) Carrington, A.; McLachlan, A. D. *Introduction to Magnetic Resonance*; Chapman and Hall: London, 1979; p 179.
(37) McConnell, H. M. *J. Chem. Phys.* **1956**, *24*, 764−766.
(38) McConnell, H. M.; Chestnut, D. B. *J. Chem. Phys.* **1958**, *28*, 107−117.
(39) Atherton, N. M. *Electron Spin Resonance Theory and Applications*; Ellis Horwood Limited: Chichester, U.K.; Halsted Press: John Wiley & Sons Inc.: New York, 1993.
(40) Bender, C. J.; Sahlin, M.; Babcock, G. T.; Barry, B. A.; Chandrashekar, T. K.; Salowe, S. P.; Stubbe, J.; Lindström, B.; Petersson, L.; Ehrenberg, A.; Sjöberg, B.-M. *J. Am. Chem. Soc.* **1989**, *111*, 8076−8083.
(41) Heller, C.; McConnell, H. M. *J. Chem. Phys.* **1960**, *32*, 1535−1539.

$\rho^{\pi}_{C1'}$ is the π-electron spin density at C1′. The dipolar part, $\mathbf{D}^{H_\beta}_{C}$, is small due to the relatively large distance between C1′ and the β-protons and is given in millitesla by[24]

$$\mathbf{D}^{H_\beta}_{C} = \begin{bmatrix} 0.07 & & \\ & -0.03 & \\ & & -0.04 \end{bmatrix} \rho^{\pi}_{C1'} \qquad (4)$$

The influence of a conformational variety on the dipolar couplings is assumed to be minor, and therefore, we may use the dipolar tensor of eq 4 as an average interaction for each conformation. Since the magnitude of the γ-proton hfi is very small,[21,43] this interaction was neglected in our simulations.

^{2}H-Hyperfine Interactions. In powder EPR spectroscopy, the spectrum is broadened due to the anisotropic, dipolar (proton) hfi, which in combination with *g* anisotropy makes it often impossible to resolve each individual hfi in the EPR spectrum. We therefore used selective proton/deuteron exchange, which results in a reduction of the selected proton hfi magnitude by a factor of about 6 (γH = 267 522 rad·s^{-1}·mT^{-1}, γ_D = 41 065 rad·s^{-1}·mT^{-1}, resulting in g_H/g_D = 6.515[44]).

^{13}C-Hyperfine Interactions. The magnitude and sign of an ^{13}C-hfi are sensitive functions of the spin distribution. In particular, they strongly depend on the spin densities of neighboring atoms and on structural changes of the molecular framework.[45] Dipolar ^{13}C-hyperfine couplings are determined by the spin density at the labeled carbon and by the spin density at the neighboring atoms X. The role of the neighboring atoms will become more important when the spin density at these atoms is high and/or when it is low at the labeled atom. For a ^{13}C-dipolar hyperfine coupling, two distinct approximations can be used: the "central-atom" and the "non-central-atom" approximation. The central-atom approximation holds for high spin density at the labeled carbon, which then mainly determines the anisotropy of the ^{13}C-hfi. Due to the odd-alternate character of the tyrosine radical, other neighboring interactions can be neglected because of their low spin density. In this case, the dipolar coupling tensor for an unpaired electron in a p orbital centered on the ^{13}C atom is given in millitesla by[39,46]

$$\mathbf{D}_C = \begin{bmatrix} -3.83 & 0.00 & 0.00 \\ 0.00 & -3.83 & 0.00 \\ 0.00 & 0.00 & 7.66 \end{bmatrix} \rho^{\pi}_{C} \qquad (5)$$

For a low spin density at the ^{13}C-labeled carbon position, the non-central-atom approximation holds. Here, besides the unpaired electron density at the labeled carbon, the unpaired electron density at neighboring atoms X is important. The determination of this part of the dipolar coupling, $\mathbf{D}_{CX_i}$, requires a summation over all interacting neighbor atoms X_i.[39] The total dipolar ^{13}C-hfi in the non-central-atom approximation is then given by

$$\mathbf{D}^{C}_{total} = \mathbf{D}_C + \mathbf{D}_{CX_i} \qquad (6)$$

whereas the total hyperfine tensor is given by

$$\mathbf{A}^{C}_{total} = \mathbf{A}^{C}_{isotropic} + \mathbf{D}^{C}_{total} \qquad (7)$$

In comparison with isotropic proton hfi, the theory of isotropic ^{13}C-hfi is more complicated, although the basic principles are the same. The treatment by Karplus and Fraenkel, which is based on valence bond theory,[47] has been proven useful for accurately determining spin densities for several ^{13}C-labeled sp^2-hybridized π-electron radicals such as semiquinone radical species.[45,47−49] Magnitude and sign of the isotropic ^{13}C-hfi are relatively easily determined. The net unpaired spin density at the nucleus C arises from mixing of the σ and π electrons through exchange interactions in the molecular orbitals resulting in a total isotropic splitting produced by the nucleus of this (sp^2-hybridized) carbon atom C and its neighbor atoms X_i (i = 1−3) which is given by

$$A^{C}_{C} = (S^{C} + \sum_{i=1}^{3} Q^{C}_{CX_i})\rho^{\pi}_{C} + \sum_{i=1}^{3} Q^{C}_{X_iC}\rho^{\pi}_{i} \qquad (8)$$

where ρ^{π}_{C} and ρ^{π}_{i} are the π-electron spin densities at the atoms C and X_i, respectively.[47] The contribution of the 1s electrons is determined by S^C and that of the 2s electrons by the *Q*'s. Here *Q* denotes a proportionality constant comparable to that introduced by McConnell for proton hfi (see eq 1). Application of this formula for tyrosine radicals provides a method to calculate easily magnitude and sign of the isotopic ^{13}C-hfi when the appropriate *Q* values for the $\sigma-\pi$ exchange interactions in a particular bond are known. The *Q* values used here for C−H and C−C bonds were estimated from calculations of the $\sigma-\pi$ interactions in a planar CHC_2 fragment and are −1.27, 1.444, −1.394, and 1.95 mT for S^C, $Q^{C}_{CC'}$, $Q^{C}_{C'C}$, and Q^{C}_{CH}, respectively.[47] These parameters are valid for carbon atoms with equivalent sp^2-hybrid bonds and a C−C bond length of 1.38 Å. The Karplus−Fraenkel theory then gives

$$A^{C}_{C} = 3.56\rho^{\pi}_{C} - 1.39(\rho^{\pi}_{C'} + \rho^{\pi}_{C''}) \qquad (9)$$

and

$$A^{C}_{C} = 3.06\rho^{\pi}_{C} - 1.39(\rho^{\pi}_{C'} + \rho^{\pi}_{C''} + \rho^{\pi}_{C'''}) \qquad (10)$$

for the ^{13}C splitting in millitesla of a carbon atom C bonded to two other carbon atoms, C′ and C″, and a hydrogen atom, and of a carbon atom bonded to three other carbons, C′, C″, and C‴, respectively. If the carbonyl carbon atom C is bonded to an oxygen atom O and two other carbons atoms (C′ and C″), the carbonyl ^{13}C splitting is given by

$$A^{C}_{CO} = 1.62\rho^{\pi}_{C} - 1.39(\rho^{\pi}_{C'} + \rho^{\pi}_{C''}) + Q^{C}_{CO}\rho^{\pi}_{C} + Q^{C}_{OC}\rho^{\pi}_{O} \qquad (11)$$

There is some uncertainty in the $\sigma-\pi$ polarization parameters for the C−O bond, Q^{C}_{CO} and Q^{C}_{OC}. Both parameters seem to depend on the magnitude of the McConnell Q^{H}_{CH} parameter.[50] Magnitudes of the reported Q^{C}_{CO} and Q^{C}_{OC} values in the literature vary between 0.87 and 1.92 mT for Q^{C}_{CO} and between −3.22 and 1.04 mT for Q^{C}_{OC}. Following Broze and Luz, who studied an extensive array of semiquinones, we used Q^{C}_{CO} = 3.60 mT and Q^{C}_{OC} = −2.43 mT.[51]

^{17}O-Hyperfine Interactions. Since ^{16}O has no nuclear magnetic moment, the spin density at the phenol oxygen atom in the tyrosine radical must be determined by isotope substitu-

(42) Fessenden, R. W.; Schuler, R. H. *J. Chem. Phys.* **1963**, *39*, 2147−2195.
(43) Underwood, G. R.: Vogel, V. L. *J. Am. Chem. Soc.* **1971**, *93*, 1058−1063.
(44) Kurreck, H.; Kirste, B.; Lubitz, W. *Electron Nuclear Double Resonance Spectroscopy of Radicals in Solution*; VCH Publishers Inc.: New York, 1988.
(45) Fraenkel, G. K. *Pure Appl. Chem.* **1962**, *4*, 143−156.
(46) Morton, J. R.; Preston, K. F. *J. Magn. Reson.* **1978**, *30*, 577−582.
(47) Karplus, M.; Fraenkel, G. K. *J. Chem. Phys.* **1961**, *35*, 1312−1323.
(48) Bolton, J. R.; Fraenkel, G. K. *J. Chem. Phys.* **1964**, *40*, 3307−3320.
(49) Strauss, H. L.; Fraenkel, G. K. *J. Chem. Phys.* **1961**, *35*, 1738−1750.
(50) Das, M. R.; Fraenkel, G. K. *J. Chem. Phys.* **1965**, *42*, 1350−1360.
(51) Broze, M.; Luz, Z. *J. Chem. Phys.* **1969**, *51*, 738−753.

tion. For the stable ^{17}O isotope $I = {}^5/_2$, resulting in a 6-fold splitting of the EPR lines. The intensity of the ^{17}O satellites is therefore relatively small, the more so because at best 50% enrichement in ^{17}O can be achieved in practice (in our case 43%). The ^{17}O-hfi can be interpreted similarly to the ^{13}C-hfi, and by analogy with eq 8 we can write for the isotropic ^{17}O-hfi

$$A_O^O = Q_{OC}^O \rho_{O4'}^\pi + Q_{CO}^O \rho_{C4'}^\pi \qquad (12)$$

where $\rho_{O4'}^\pi$ and $\rho_{C4'}^\pi$ are the spin densities in the p orbitals of the phenol oxygen O4′ and neighboring carbon C4′, respectively, and the Q's are $\sigma-\pi$ interaction parameters. The parameter Q_{OC}^O is a measure of the electron spin polarization in the s orbitals of the ^{17}O nucleus due to spin density in the p orbital of the oxygen atom itself. Q_{CO}^O represents the polarization due to the spin density at C4′. In the literature, Q_{OC}^O varies from -3 to -11 mT and Q_{CO}^O varies from -2 to $+2$ mT.[51,52] Though eq 12, with $Q_{OC}^O = -4.0 \pm 0.5$ mT and $Q_{CO}^O = 0$ mT, has been proven a good approximation for a number of carbonyl radicals,[53] both Q's strongly depend on the type of radical making it difficult to determine spin densities from this equation. On the other hand, $\rho_{O4'}^\pi$, is more directly deduced from the ^{17}O-dipolar coupling tensor $\mathbf{D}_O$ calculated for an unpaired electron in a p orbital centered on the atom:[39,46]

$$\mathbf{D}_C^{H_\beta} = \begin{bmatrix} 6.01 & 0.00 & 0.00 \\ 0.00 & 6.01 & 0.00 \\ 0.00 & 0.00 & -12.0 \end{bmatrix} \rho_{O4'}^\pi \qquad (13)$$

Note that as a result of the negative gyromagnetic moment of the ^{17}O nucleus, the sign of the tensor elements in eq 13 is different from that in eq 5.

Results and Discussion

Photochemical oxidation of tyrosine in alkaline solution creates a neutral tyrosine π-radical.[54−57] In frozen solution, EPR spectra are anisotropically broadened, by g anisotropy and partially resolved (anisotropic) hyperfine structure from proton interactions with the unpaired electron. Well-determined values for the g matrix and proton hfi are thus a prerequisite for accurate line shape simulations of the spectra of ^{13}C and ^{17}O samples, from which the principal elements of the ^{13}C- and ^{17}O-hfi tensors are derived. The spin-density distribution follows most directly from the dipolar part of the anisotropic ^{13}C- and ^{17}O-hfi, which is extracted from the hfi tensor by subtracting the isotropic part. Additional structural information is obtained from proton hfi, which also serve as a check on the spin densities calculated from the ^{13}C-hfi data.

The *g* Matrix. An important observable related to the electronic structure of the neutral tyrosine radical is the g matrix. According to the g matrix theory of Stone,[58,59] the out-of-plane g component of planar hydrocarbon π-radicals is equal to the free-electron value, g_e, whereas the in-plane components are generally shifted to higher values due to spin−orbit coupling. More recent calculations including a relativistic mass correction show that for planar aromatics a small negative shift relative to the free electron value g_e may occur for the g component perpendicular to the molecular plane.[60] Large deflections from g_e, however, can be excluded for this type of radicals. The principal axes of the g matrix of the tyrosine radical are defined as follows: g_{xx} is parallel with the line through C1′−C4′−O4′, g_{zz} is perpendicular to the aromatic ring, coinciding with the axis of the p_z atomic orbital, and the g_{yy} axis is perpendicular to the other two axes (see Figure 1). The principal g-matrix components of the neutral tyrosine π-radical generated by UV photolysis in frozen solution were found from simulation of the spectrum of perdeuterated tyrosine recorded at Q-band (Figure 2, lower right spectrum): $g_{xx} = 2.0068 \pm 0.0002$, $g_{yy} = 2.0043 \pm 0.0002$, and $g_{zz} = 2.0023 \pm 0.0002$. The relatively low g_{xx} value indicates strong hydrogen bond interactions, with an average bond length of about 1.6 Å, with the environment.[61] The three principal g values are in good agreement with values determined for the tyrosine radical in crystals of L-tyrosine: $g_{xx} = 2.0067 \pm 0.0005$, $g_{yy} = 2.0045 \pm 0.0005$, and $g_{zz} = 2.0023 \pm 0.0005$.[16] The resulting isotropic g value of the neutral tyrosine radical ($g_{iso} = 2.0045 \pm 0.0002$) corresponds well with literature values from X-band studies[16,21] and provides conclusive evidence that a neutral tyrosine radical was created by UV irradiation, and that, as distinct from room-temperature experi-

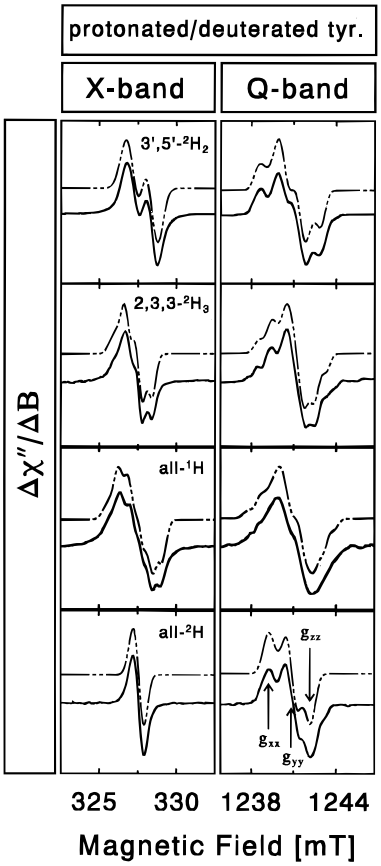

Figure 2. Experimental (solid line) and simulated (dashed line) X- and Q-band spectra of [3′,5′-$^2H_2$]-, [2,3,3-$^2H_3$]-, all-^1H- and all-^2H-tyrosine radicals in alkaline (NaOH pH11) frozen solution. For X-band (9.183 GHz): modulation amplitude = 0.025 mT, scan speed = 0.167 mT/min, time constant = 3 s, microwave power = 50 μW, temperature = 90 K. For Q-band (34.808 GHz): modulation amplitude = 0.25 mT, scan speed = 1 mT/min, time constant = 1 s, microwave power = 1 μW, temperature = 100 K, five scans average.

(52) Broze, M.; Luz, Z.; Silver, B. L. *J. Chem. Phys.* **1967**, *46*, 4891−4902.
(53) Gulick, W. M., Jr.; Geske, D. H. *J. Am. Chem. Soc.* **1966**, *88*, 4119−4124.
(54) DeFilippis, M. R.; Murthy, C. P.; Faraggi, M.; Klapper, M. H. *Biochemistry* **1989**, *28*, 4847−4853.
(55) DeFilippis, M. R.; Murthy, C. P.; Broitman, F.; Weintraub, D.; Faraggi, M.; Klapper, M. H. *J. Phys. Chem.* **1991**, *95*, 3416−3419.
(56) Land, E. J.; Porter, G.; Strachan, E. *Trans. Faraday Soc.* **1960**, *57*, 1885−1893.
(57) Creed, D. *Photochem. Photobiol.* **1984**, 563−575.
(58) Stone, A. J. *Proc. R. Soc. Chem.* **1963**, *A271*, 424.
(59) Stone, A. J. *Mol. Phys.* **1963**, *6*, 509−515.
(60) Angstl, R. *Chem. Phys.* **1989**, *132*, 435−442.
(61) Un, S.; Tang, X.-S.; Diner, B. A. *Biochemistry* **1996**, *35*, 679−684.

Table 1. ^{1}H-, ^{13}C-, and ^{17}O-Hyperfine Interactions,[a] Euler Angle ϕ,[b] and g Values[c] of the Neutral Tyrosine Radical in Frozen Solution

hfi	A_{xx} (mT)	A_{yy} (mT)	A_{zz} (mT)	A_{iso} (mT)	A_{K-F}[d] (mT)	A_{K-F}[e] (mT)	ϕ
C2′−H	0.17	0.27	0.04	0.16			30
C3′−H	−0.96	−0.28	−0.70	−0.64			−23
C5′−H	−0.96	−0.28	−0.70	−0.64			23
C6′−H	0.17	0.27	0.04	0.16			−30
C1′−$H_{\beta 1}$[f]	0.15	0.11	0.11	0.12			0
C1′−$H_{\beta 2}$[f]	0.95	0.92	0.92	0.93			0
1′-^{13}C	−0.30	−0.30	3.40	0.93	1.09	0.90	0
2′-^{13}C	−0.65	−0.80	−1.20	−0.88	−0.91	−0.88	30
3′-^{13}C	−0.60	−0.60	2.00	0.27	0.80	0.67	−23
4′-^{13}C	−1.10	−1.20	−0.65	−0.98	−1.16	−1.04	0
5′-^{13}C	−0.60	−0.60	2.00	0.27	0.80	0.67	23
4′-^{17}O	0.50	0.70	−4.07	−0.96	−1.04		0

$g_{xx} = 2.0068 \pm 0.0002$ $g_{yy} = 2.0043 \pm 0.0002$ $g_{zz} = 2.0023 \pm 0.0002$

[a] Hfi obtained from the simulation of EPR spectra at 9.2 and 34.8 GHz. Estimated errors vary between 0.02 and 0.07 mT. [b] Euler angle as defined in Figure 1; the other angles, θ and ψ, were always set to zero. The sign is taken positive for a clockwise rotation. Note that the EPR simulation does not distinguish between positive and negative angles. [c] g values obtained from the simulation of the spectrum shown in Figure 2 lower right corner. [d] Isotropic ^{13}C-hfi determined from the Karplus−Fraenkel theory with $S^{C} = -1.27$ mT.[47] [e] Isotropic ^{13}C-hfi determined from the Karplus−Fraenkel theory with $S^{C} = -1.875$ mT.[87] [f] Values corresponding to fixed dihedral angles of 75° and 45°, respectively, and a spin density of 0.32 at C1′.

ments,[22] no other radicals, such as dopa-derived radicals ($g_{iso} = 2.0021$) or a $CO_2^{\bullet-}$ radical ($g_{iso} = 2.0001$), were present. Solvent radicals such as $O^{\bullet-}$ and $SO_4^{\bullet-}$, as reported by Moan et al.,[62] were neither observed. We also note that the g values of the neutral tyrosine radical in vitro are close to those found for the $Y_D^{\bullet}$ tyrosine radical in reaction centers of Photosystem II of plants.[63]

Hyperfine Interactions. Figure 2 shows experimental X- and Q-band spectra of selectively deuterated, fully deuterated and fully protonated tyrosine radicals (solid lines), together with simulated line shapes (dashed lines). The recorded X-band spectra are virtually identical with the spectra reported by Barry et al.[19] The additional Q-band spectra allowed more accurate calculation of the major ^{1}H-hfi. All ^{1}H-hfi and other parameters obtained from the simulations are tabulated in Table 1. The estimated errors of the individual ^{1}H-hfi are based on the sensitivity of the *eight* spectra to changes in the hfi parameter set. The present "best" set of the in vitro neutral tyrosine radical proton hfi is the result of extensive searches in parameter space and agrees well with hfi estimated from theoretical considerations,[64,65] and for the α-proton hfi, with values obtained from ESEEM studies.[17]

Figure 3 shows experimental (solid lines) and simulated (dashed lines) X- and Q-band EPR spectra of a variety of ^{13}C-labeled neutral tyrosine radicals with and without ^{2}H-labeling at the positions 3′ and 5′. The simulations were carried out using the parameters derived from the set of EPR spectra of ^{1}H- and ^{2}H-tyrosines of Figure 2. Note that for each ^{13}C-labeled sample four spectra had to be simulated with identical ^{13}C-hfi tensors, namely spectra recorded at two frequencies (9.2 or 34.8 GHz) and with two different protonation states (with or without 3′, 5′ deuteration).

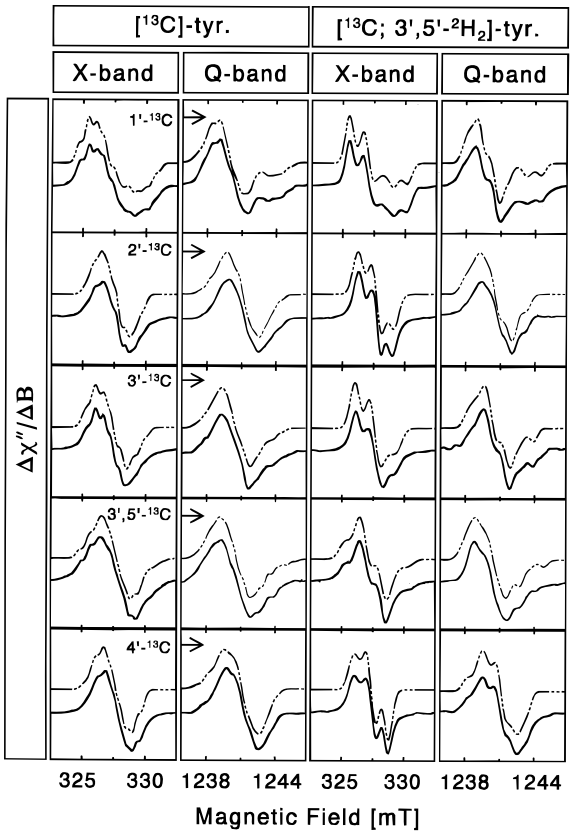

Figure 3. Experimental (solid line) and simulated (dashed line) X- and Q-band spectra of ^{13}C-labeled tyrosine radicals in alkaline (NaOH, pH 11) frozen solution. Upper four spectra: [1′-$^{13}C_1$]tyrosine and [1′-$^{13}C_1$,3′,5′-$^{2}H_2$]tyrosine. Second row: [2′-$^{13}C_1$]tyrosine and [2′-$^{13}C_1$,3′,5′-$^{2}H_2$]tyrosine. Third row: [3′-$^{13}C_1$]tyrosine and [3′-$^{13}C_1$,3′,5′-$^{2}H_2$]tyrosine. Fourth row: [3′,5′-$^{13}C_2$]tyrosine and [3′,5′-$^{13}C_2$,3′,5′-$^{2}H_2$]tyrosine. Lowest row: [4′-$^{13}C_1$]tyrosine and [4′-$^{13}C_1$,3′,5′-$^{2}H_2$]tyrosine. Experimental conditions as described at Figure 2.

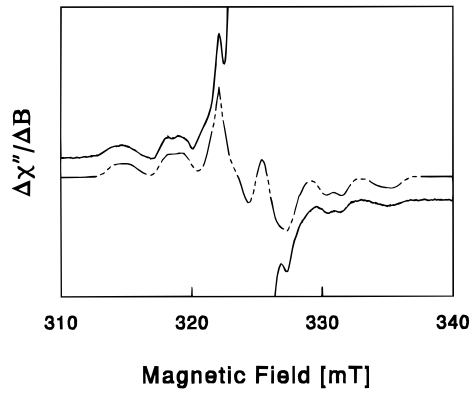

Figure 4. Experimental (solid line) and simulated (dashed line) X-band (9.183 GHz) spectra of [4′-$^{17}O_1$,3′,5′-$^{2}H_2$]tyrosine radicals in alkaline (NaOD, pH 11) frozen solution; modulation amplitude = 0.25 mT, scan speed = 5 mT/min, time constant = 1 s, microwave power = 50 μW, temperature = 90 K. The central part of the spectrum due to unlabeled tyrosine is left out.

Figure 4 shows the experimental (solid line) and simulated (dashed line) X-band EPR spectra of the [4′-$^{17}O_1$,3′,5′-$^{2}H_2$]-tyrosine radical.

The hfi tenors obtained from the line shape simulations of the ^{13}C and ^{17}O enriched samples are summarized in Table 1 and are in good agreement with calculated couplings for hydrogen-bonded tyrosine radicals.[65,66]

Spin Densities. With the aid of the hfi for the variously labeled tyrosines collected in Table 1, we shall now analyze

(62) Moan, J.; Kaalhus, O. *J. Chem. Phys.* **1974**, *61*, 3556−3566.
(63) Un, S.; Atta, M.; Fontecave, M.; Rutherford, A. W. *J. Am. Chem. Soc.* **1995**, *117*, 10713−10719.
(64) O'Malley, P. J.; MacFarlane, A. J.; Rigby, S. E. J.; Nugent, J. H. A. *Biochim. Biophys. Acta* **1995**, *1232*, 175−179.
(65) O'Malley, P. J.; Ellson, D. *Biochim. Biophys. Acta* **1997**, in press.

the spin density at each carbon position of the aromatic ring and at the 4′-oxygen.

Position C1′. Deuteration of the 3′ and 5′ positions ([3′,5′-$^2H_2$]tyrosine) reduces the large proton hfi at these positions by a factor of about 6. Now, the spectral shape is determined largely by one of the β-proton hfi (Figure 2), which is positive in sign (eq 3) and entirely determined by the spin density at C1′. Due to the conformational distribution of the β-protons,[24] their isotropic hfi vary in the range of 0−0.5 mT ($90° < \theta_1 < 60°$) and 0.5−1.5 mT ($60° < \theta_2 < 30°$), making it difficult to fix the spin density at this position from the measured isotropic proton hfi. Furthermore, the r^{-3} dependence of the dipolar part of the interaction and the relatively long distance r from the center of the p_z orbital at C1′ makes the anisotropic proton hfi relatively small and unsuitable for determining $\rho^{\pi}_{C1'}$. In contrast, a ^{13}C label placed at the C1′ position ([1′-$^{13}C_1$]tyrosine) induces a large ^{13}C-hfi in the z direction, indicating high spin density at this position (Figure 3). The ^{13}C-hyperfine parameters obtained from spectral simulations are $A^C_{xx} = A^C_{yy} = 0.13$ mT and $A^C_{zz} = 3.43$ mT (Table 1). Because the spin density at the neighboring atoms C2′ and C6′ is small (see below), their influence is negligible. Applying the central-atom approximation, the observed dipolar splittings directly yield a spin density of 0.32 at C1′. The narrow lines of the observed [1′-$^{13}C_1$]-tyrosine spectra provide additional proof for the suggestion of Warncke et al. that there is no significant distribution of the spin density at C1′.[24] Thus, the distribution of the β-proton hfi is caused by conformational variations only.

Positions C3′ and C5′. When both methylene β-protons are deuterated ([2,3,3-$^2H_3$]tyrosine) the spectral shape results mainly from the hfi with the protons at positions 3′ and 5′ (Figure 2). The proton hyperfine tensor components for the positions 3′ and 5′ obtained from the simulations, $A_{xx} = -0.96$ mT, $A_{yy} = -0.28$ mT, and $A_{zz} = -0.70$ mT, exhibit the rhombic pattern common for α-protons,[67] but reflect a tensor that is *not* exactly collinear with the C−H bond.[16,20] Normally, assuming a regular hexagonal aromatic ring structure, one would expect an angle ϕ of 30° instead of 23° ± 2°, where ϕ is the Euler angle transforming the hyperfine components, defined in the molecular system, to the g-axes system (see Figure 1). This deviation from the C−H bond direction could possibly result from interactions with electrons at neigboring carbon or oxygen atoms.[68,69] However, calculations of electron dipolar interactions between the spin density at the phenoxy oxygen and protons 3′ and 5′ indicate that only a small deflection of about 2−3° is possible. Because no proper simulations could be obtained with an Euler angle ϕ close to 30°, the relatively large deflection may result from a change in bond angle of the C−H proton, due to steric hindrance, or from a ring structure distortion. A similar deflection has been reported for semiquinone radicals.[68,69] Since we expect the tyrosine radical to be planar, the other Euler angles, θ and ψ, are chosen zero although an out-of-plane proton orientation of 10−15° cannot be definitely excluded at this stage of our analysis.[70] Larger out-of-plane orientations cause direct overlap of the proton s orbital with the p_z orbital of the neighboring carbon and will drastically increase the magnitude of the isotropic proton hfi.[70] Deviations of the whole π-system from planarity have only a moderate effect on the coupling constants of the α-protons.[71]

Our proton hfi tensor for the position 3′ and 5′ agree well with the ^2H couplings obtained from ESEEM spectroscopy of 3′,5′ deuterated tyrosine radicals in frozen alkaline solution.[18] The relatively large magnitudes of the isotropic hfi reflect a high spin density at C3′ and C5′, which must be positive in sign because large negative spin densities are very unlikely. Thus, according to the McConnell relation (eq 1), the proton hfi must be negative and the tentative spin densities at the carbons C3′ and C5′ are $\rho^{\pi}_{C3'} = \rho^{\pi}_{C5'} = +0.26$.

We can derive more precise information from the ^{13}C-hfi obtained from the simulations of the four measured spectra of [3′-$^{13}C_1$]tyrosine radicals (Figure 3). The ^{13}C-hfi for position C3′ are tabulated in Table 1. Following the odd-alternate spin density pattern, the spin density at the neighboring atoms can be neglected and from the observed anisotropy a density of 0.23 is deduced by using eq 5. The ^{13}C-hyperfine tensor is chosen collinear to the proton hyperfine axes, in accordance with ^{13}C-EPR results on malonic acid crystals.[72] In comparison to protons, ^{13}C-hfi have a much larger angular dependence and serve therefore as a better tool for structure determination. The magnitude of the observed ^{13}C-hfi indicates that the hydrogen atoms are situated in the plane of the aromatic ring. Any perturbation of the sp^2-hybridization will severely influence the ^{13}C-hfi.[47] For instance, an out-of-plane angle of 10° will result in a very large isotropic hyperfine coupling of 3 mT and a 15° out-of-plane angle will even give a 5 mT interaction for a spin density of 0.23. The effects of in-plane alterations have been discussed by Strauss and Fraenkel.[49] Both the Q^H_{CH} and the Q^C_{CH} $\sigma-\pi$ interaction parameters will change considerably upon variation of the C2′−C3′−C4′ angle. A small deviation from the C2′−C3′−C4′ angle of 120° assumed in the theory, may therefore explain the difference (0.26 vs 0.23) in the observed spin density at C3′.

The experimental spectra of the double ^{13}C-labeled tyrosine radicals ([3′,5′-$^{13}C_2$]tyrosine), shown in Figure 3, could be well simulated with equal ^{13}C-hyperfine parameters for C3′ and C5′: $A^C_{xx} = A^C_{yy} = -0.50$ mT and $A^C_{zz} = 1.90$ mT. This supports the above determination of the hyperfine tensor components, and indicates that there is no large difference in the spin density for these two positions of the neutral in vitro tyrosine radical. Electron nuclear double resonance (ENDOR) studies on neutral tyrosine radicals in photosynthetic reaction centers of various cyanobacteria[73] and EPR studies on tyrosine/HCl crystals[17] suggest that the proton 3′ and 5′ hfi, and thus the corresponding spin densities, are inequivalent ($\Delta\rho \approx 0.02$). In contrast, ESEEM of [3′,5′-$^2H_2$]-L-tyrosine radicals in frozen solution yields $\Delta\rho < 0.01$.[18] Theoretically it has been shown that an asymmetric orientation of the aromatic ring relative to the β-protons,[73] asymmetry of the side chain[15] or hydrogen bonding[74] could be responsible for an inequivalence. Within the accuracy of our experiments ($\Delta\rho \approx 0.01$), however, we cannot distinguish $\rho^{\pi}_{C3'}$ and $\rho^{\pi}_{C5'}$ for the neutral tyrosine radical in frozen solution.

Room-temperature NMR results show that there is a dynamic 180° flip of the aromatic ring.[75] Since the EPR spectra of the [3′-$^{13}C_1$]- and [3′,5′-$^{13}C_2$]-labeled tyrosine radicals are different, we conclude that the aromatic ring does not experience fast 180°

(66) Himo, F.; Gräslund, A.; Eriksson, L. A. *Biophys. J.* **1997**, *72*, 1556−1567.
(67) McConnell, H. M.; Heller, C.; Cole, T.; Fessenden, R. W. *J. Am. Chem. Soc.* **1960**, *82*, 766−775.
(68) O'Malley, P. J.; Babcock, G. T. *J. Am. Chem. Soc.* **1986**, *108*, 3995−4001.
(69) Burghaus, O.; Plato, M.; Rohrer, M.; Möbius, K. *J. Phys. Chem.* **1993**, *97*, 7639−7647.
(70) Karplus, M. *J. Chem. Phys.* **1959**, *30*, 15−18.
(71) Gerson, F.; Lamprecht, A.; Scholz, M.; Troxler, H. *Helv. Chim. Acta* **1996**, *79*, 307−318.
(72) Cole, T.; Heller, C. *J. Chem. Phys.* **1961**, *34*, 1085−1086.
(73) Rigby, S. E. J.; Nugent, J. H. A.; O'Malley, P. J. *Biochemistry* **1994**, *33*, 1734−1742.
(74) Hoganson, C. W.; Sahlin, M.; Sjöberg, B.-M.; Babcock, G. T. *J. Am. Chem. Soc.* **1996**, *118*, 4672−4679.

flips on the EPR time scale at the low temperature of the measurements (<100 K).

Position C2′ and C6′. The EPR spectrum hardly changes upon deuteration due to the low spin density at these positions.[19] This makes it difficult to determine the magnitude, sign, and orientation of the corresponding proton hyperfine tensor elements. The principal elements of the proton hfi tensor for the positions 2′ and 6′ resulting from our simulations are similar to values reported by Hoganson and Babcock.[20] The magnitude of the spin densities at the positions C2′ and C6′, determined from the corresponding isotropic proton hfi, is about 0.06 (eq 1). As a consequence of the low spin density there is uncertainty in the precise orientation of the hyperfine tensor with respect to the *g* axes. We have chosen an Euler angle ϕ of $\pm 30°$. Other angles cannot be excluded but the impact of ϕ different from 30°, for example $\phi = 23°$, on the small proton hfi at C2′ and C6′ and therefore on the spectral line shape is minor. EPR experiments of neutral tyrosine radicals in solution show that the isotropic hfi at these positions are both about 0.15 mT.[21] ENDOR studies of the tyrosine $Y_D^{\bullet}$ radical in Photosystem II reaction center proteins indicate that, as with the 3′ and 5′ positions, the electron spin densities at the 2′ and 6′ positions may not be equivalent ($\Delta\rho \approx 0.01 \pm 0.01$).[73]

Despite the low spin density at the C2′ position, an additional ^{13}C-hyperfine splitting is clearly seen in the EPR spectra of the [2′-^{13} C_1,3′,5′-$^2H_2$]tyrosine radical (Figure 3). This relatively large, nearly isotropic ^{13}C-hfi results from interactions with the high spin density at the neighboring carbon atoms, C1′ and C3′. The principal values of the ^{13}C-hfi tensor are: $A^C_{xx} = -0.60$ mT, $A^C_{yy} = -0.70$ mT, and $A^C_{zz} = -1.17$ mT, with the sign found from the Karplus−Fraenkel relations. The axes for the tensor are again chosen collinear with the proton hfi tensor axes. Knowing the spin density at C1′ and C3′, we can determine the spin density at C2′ by using eq 6. The *x* and *y* coordinates required to calculated the dipolar interactions from the neighboring carbons follow from computationally predicted geometrical structures of the tyrosine[64] and phenoxyl radical,[10] and from neutron diffraction experiments on tyrosine crystals.[76] The π-electron spin-density distribution at the carbon atom is represented by two point spins located at $z = \pm 0.77$ Å, the average distance of the π-electron clouds with respect to the phenoxyl ring, with each cloud carrying half the spin density of the carbon atom.[77] The point spin representation, the geometry and the bond lengths used for calculating the $\mathbf{D}_{CX}$ tensors are depicted in Figure 5. The dipolar tensors resulting from an interaction with spin density located at C1′ and C3′ can now be determined. Equation 6 then gives three equations for the three principal elements of $\mathbf{D}^C_{total}$, with $\rho^{\pi}_{C2'}$ as a single variable, which yield a value of $\rho^{\pi}_{C2'} = -0.04$ as best solution. The negative sign reflects a spin polarization opposite to the net spin polarization of the radical.[45] Here again, ^{13}C probes are shown to be powerful tools: small spin densities and their sign are easily determined. Since the [6′-$^{13}C_1$]-labeled tyrosine radical was not available, we could not determine the spin density at the C6′ position and have assumed that it is equal to that at C2′, the inequivalency being within the error of our experiments ($\Delta\rho \approx 0.01$).

Position C4′. Since this is a "blind" position, i.e., it lacks proton attachement, proton hfi are absent and ^{13}C-labeling of the C4′ position ([4′-$^{13}C_1$]tyrosine) is necessary to determine the spin density. The ^{13}C-hfi resulting from the simulations of the four spectra in Figure 3 are tabulated in Table 1. The sign of the ^{13}C-hfi obtained, $A^C_{xx} = -1.00$ mT, $A^C_{yy} = -0.98$ mT, and $A^C_{zz} = -0.68$ mT, follows from the Karplus−Fraenkel theory (eq 11). In this case, interpretation of the ^{13}C-hfi obtained for this position is more difficult since we do not know the exact spin density at the phenol oxygen O4′. Because the spin density at the O4′ is expected to be high, it certainly will influence the anisotropic ^{13}C-hyperfine couplings for C4′. Nevertheless we will first analyze the spectra without using the data for the ^{17}O-labeled sample, and show that a consistent set of spin densities for C4′ *and* O4′ can be derived from the ^{13}C couplings only. These results are then confronted with the direct determination of the spin density at the phenol oxygen by using ^{17}O-labeled tyrosine radicals, and it is shown that very good agreement is obtained. If we assume that $\rho^{\pi}_{C2'} = \rho^{\pi}_{C6'}$ and $\rho^{\pi}_{C3'} = \rho^{\pi}_{C5'}$, then it follows from the conservation condition, $\sum\rho^{\pi}_i = 1$, that the sum of the spin densities located at O4′ and C4′ is 0.30. With the known spin densities at C3′ and C5′, together with the ^{13}C-hfi anisotropy for position C4′, eq 6 for the non-central-atom approximation gives $\rho^{\pi}_{C4'} = 0.05$ and $\rho^{\pi}_{O4'} = 0.25$ as best solution. All the coordinates required for calculating the $\mathbf{D}_{CX}$ tensors are given in Figure 5. The C−O bond length is chosen to be 1.25 Å, in the lower range of the C−O distances resulting from various geometry optimization procedures for phenoxyl radicals, viz. 1.22−1.38 Å.[10] Larger C−O distances, corresponding to more single-bond character, however, cannot be excluded because a change of bond length to 1.40 Å has little influence on the magnitude of the dipolar couplings. The relatively high spin density at O4′ and the fact that the spin density at C4′ has positive sign indicate that there is appreciable delocalization of the unpaired electron, which can be explained by a relatively short C−O bond. Ultraviolet resonance Raman spectroscopy experiments on ^{17}O-labeled phenoxyl radicals,[78] as well as several structural geometries calculated recently by O'Malley et al.[64,65] and Qin and Wheeler,[15] also indicate that the C−O bond in the neutral tyrosine radical has double-bond character.

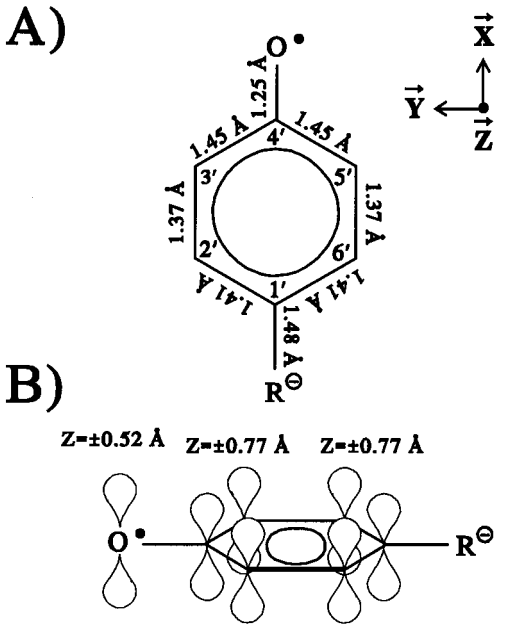

Figure 5. (A) Geometrical structure of the tyrosine neutral radical and axes system. (B) Side view with point spin representation.

(75) Neuberger, A. *Modern Physical Methods in Biochemistry*; Neuberger, A., Van Deenen, L. L. M., Eds.; Elsevier: Amsterdam, 1985; Part A, pp 57−60.

(76) Frey, M. M.; Koetzle, T. F.; Lehmann, M. S.; Hamilton, W. C. *J. Chem. Phys.* **1973**, *58*, 2547−2556.

(77) Kemple, M. D. *Multiple Electron Resonance Spectroscopy*; Dorio, M. M., Freed, J., Eds.; Plenum Press: New York, 1979; p 420.

(78) Mukherjee, A.; McGlashen, M. L.; Spiro, T. G. *J. Phys. Chem.* **1995**, *99*, 4912−4917.

Table 2. Experimental Spin Densities Obtained from ^{1}H-, ^{13}C-, and ^{17}O-hfi and Calculated Distributions for the Neutral Tyrosine Radical

	exptl ρ^{π} [a]		calcd ρ^{π}				
atom	^{1}H	^{13}C/^{17}O	SVWN[b]	Hückel[c]	SCF[d]	ROHF[e]	PWP[f]
C1′		0.32	0.29	0.24	0.31	0.33	0.38
C2′	±0.06	−0.04	−0.06	0.01	−0.07	0	−0.11
C3′	0.26	0.23	0.21	0.20	0.26	0.22	0.25
C4′		0.05	−0.01	0.07	−0.03	0.04	0.02
C5′	0.26	0.23	0.24	0.20	0.26	0.23	0.25
C6′	±0.06	−0.04	−0.06	0.01	−0.02	0	−0.11
O4′		0.26	0.36	0.26	0.28	0.17	0.32
$\sum\rho^{\pi}$		1.01	0.97	0.99	0.99	0.99	1.00

[a] This work. Error $\Delta\rho^{\pi} = \pm 0.01$ [b] Slater−Vosko−Wilk−Nusair method.[15] [c] Hückel molecular orbital theory.[16] [d] McLachlan self-consistent-field theory.[16] [e] Restricted open-shell Hartree−Fock Austin method (AM) 1.[64] [f] Perdew−Wang−Perdew'86/individual gauge of localized orbitals (IGLO) III.[66]

From previous ^{13}C-hfi experiments, a linear relationship between $\rho^{\pi}_{C4'}$ and $\rho^{\pi}_{O4'}$ was found:[79]

$$\rho^{\pi}_{C4'} = -1.115\rho^{\pi}_{O4'} + 0.3406 \qquad (14)$$

With $\rho^{\pi}_{C4'} = 0.05$ and $\rho^{\pi}_{O4'} = 0.25$, the neutral tyrosine radical fits eq 14 very well. A similar good fit was recently found for ^{13}C-labeled quinone radicals.[80]

Position O4′. From the simulation of the X-band spectrum of ^{17}O-labeled tyrosine radicals (Figure 4), the following ^{17}O-hyperfine interactions were obtained: $A^{O}_{xx} = +0.50$ mT, $A^{O}_{yy} = +0.70$ mT, and $A^{O}_{zz} = -4.07$ mT. The sign of A^{O}_{zz} must be negative due to the large negative dipolar part, i.e., a large positive spin density. A^{O}_{xx} and A^{O}_{yy}, mainly determined by the two intense peaks close to centerfield, could have a negative sign but then an isotropic ^{17}O-hfi of −1.8 mT is obtained, which value is relatively large and does not correspond with other isotropic ^{17}O-hfi values reported in the literature (for semiquinone and phenoxyl radicals, values between −0.8 and −1.1 mT were found[51−53,81,82]). In the simulation of Figure 5, quadrupole couplings, being small, were neglected and it was assumed that the oxygen was lying in the plane of the aromatic ring with the C−O bond parallel to the g_{xx} axis. We note that our EPR spectrum (Figure 4) is better resolved than that of Hoganson et al.,[74] which allowed us a more accurate determination of the ^{17}O-hyperfine elements. The isotropic value of −0.96 mT corresponds well with the values observed for phenoxyl radicals.[81,83,84] Interactions of the unpaired spin at the phenol oxygen with that at C4′, and/or H-bond formation might be responsible for the difference between A_{xx} and A_{yy}. The dipolar couplings yield a spin density of 0.26 at the phenol oxygen. This is in good agreement with the spin density obtained from our ^{13}C measurements. Neglecting the $\sigma-\pi$ polarization due to the (low) spin density at C4′, eq 13 gives us a Q^{O}_{OC} value of −3.7 mT, which is identical with the Q^{O}_{OC} value reported for phenoxyl radicals.[81]

Comparison of Experimental and Calculated Spin Densities. Table 2 and Figure 6 summarize the spin densities determined from the ^{1}H-, ^{13}C-, and ^{17}O-hfi. The spin densities

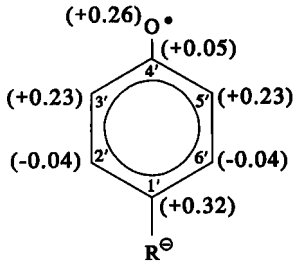

Figure 6. Overview of the spin-density distribution of the neutral tyrosine radical in alkaline frozen solution.

derived from the ^{13}C- and ^{17}O-hfi sum to 1.01. The slight deviation from unity is within experimental error and may easily be compensated by negative spin density at for instance the protons.[85] Table 2 also shows that when only proton hfi are available, one can get already a fairly good idea of the global structure and spin-density properties of the neutral tyrosine radical. For example, the odd-alternate spin density pattern becomes clearly visible, but the many assumptions and semiempirical constants involved in the relations between proton hfi and spin density make it impossible to give a complete characterization. A major uncertainty is the spin density at C1′, whose magnitude is strongly influenced by a conformational distribution of the methylene β-protons, whereas the spin densities at C4′ and O4′ are simply unknown. A much more complete and more accurate spin-density distribution is determined from the ^{13}C- and ^{17}O-hfi. This distribution is in good agreement with several computational predicted spin-density distributions published in the literature. It should be noted that the outcome of the calculations strongly depends on the chosen geometrical structure of the tyrosine radical because the spin-density distribution in a π-radical is sensitive to its geometry.[86,87] The systematically higher spin densities found from the proton hfi may indicate that the McConnell Q^{H}_{CH} value for the in vitro neutral tyrosine radical is somewhat (∼10%) larger than the value of −2.49 mT found from dipolar proton couplings for the in vivo radical[40] and may even differ for each α-proton position.[74] Since Q^{H}_{CH} also depends on the net charge on the radical,[39,48] it is obvious that spin-density determinations from observed proton splittings are not very accurate.

The Karplus−Fraenkel Theory for Isotropic ^{13}C- and ^{17}O-hfi. As we have determined the spin densities for all the phenoxyl ring atoms from their individual ^{13}C- and ^{17}O-anisotropic hyperfine components, we can apply the Karplus−Fraenkel equation as an internal check on the validity of our measured ^{13}C-hfi tensors by calculating the various isotropic ^{13}C-hfi, and comparing them with the isotropic couplings calculated from the principal tensor elements. The results are included in Table 1. For the positions C1′, C2′, and C4′, there is good agreement between the observed and calculated values. A small change of the S^{C} constant, containing the 1s contribution to the hyperfine splitting resulting from an unpaired electron in the carbon π-orbital, from −1.27 to −1.875 mT,[88] results in even better agreement (see Table 1). The observed isotropic ^{13}C-hfi for C4′ has a negative sign and is in good agreement with values found for several phenoxy radicals, despite the uncertainty in the Q^{C}_{CO} and Q^{C}_{OC} values.[81,89] For position C3′ and C5′ we see a large discrepancy between the value calculated with Karplus−Fraenkel (eq 12) and that determined from the

(79) Prabhananda, B. S.; Khakhar, M. P.; Das, M. R. *J. Am. Chem. Soc.* **1968**, *90*, 5980−5986.
(80) Kropacheva, T. N.; Van Liemt, W. B. S.; Raap, J.; Lugtenburg, J.; Hoff, A. J. *J. Phys. Chem.* **1996,** *100*, 10433−10442.
(81) Von Dimroth, K.; Berndt, F.; Volland, R.; Schweig, A. *Angew. Chem.* **1967**, *79*, 69−76.
(82) Chiu, M. F.; Sutcliffe, B. T. *Theor. Chim. Acta (Berlin)* **1970**, *16*, 331−345.
(83) Rieker, A.; Scheffler, K. *Tetrahedron Lett.* **1965**, *19*, 1337−1340.
(84) Rieker, A. *Z. Naturforsch.* **1966**, *21b*, 647−656.

(85) $|\rho_{\text{other positions}} \leq 0.03|$; M. van Hemert, private communications.

(86) Benson, H. G.; Hudson, A. *Mol. Phys.* **1971**, *20*, 185−187.
(87) Beveridge, D. L.; Guth, E. *J. Chem. Phys.* **1971**, *55*, 458−459.
(88) Reiter, R. C.; Stevenson, G. R.; Wang, Z. Y. *J. Phys. Chem.* **1990**, *94*, 5717−5720.
(89) Gilbert, L.; Kreilick, R. *J. Chem. Phys.* **1968**, *48*, 3377−3380.

trace of the ^{13}C-hfi tensor. A possible explanation for this disagreement is a change in hybridization of the atomic orbitals, as we suggested above in connection with the observed noncollinearity of the proton hyperfine tensor with the C−H bond. The Karplus−Fraenkel theory is based on an ideal regular hexagon of carbon atoms with equivalent sp^2 hybrid bonds and a C−C bond length of 1.38 Å. A distortion of this hexagonal ring will certainly lead to changes in all relevant Q values because the polarization parameters depend sensitively on the bond lengths and type of bond hybridization.[43,49] A planar distortion of several degrees has been suggested from tyrosine geometrical optimalisation computations[15,64,66] and has also been reported for phenoxy[11,12,90] and benzyl radicals.[91,92] As mentioned above, an out-of-plane distortion can be excluded, because this will destroy the sp^2-hybridized π-electron character of the tyrosine radical, which would result in totally different, much larger, ^{13}C-hfi.

Extending the Karplus−Fraenkel theory for isotropic ^{17}O-hfi results in good agreement with the experimental value if one uses the proper Q^{O}_{OC} and Q^{O}_{CO} values.

Conclusions

The full spin-density distribution in UV-generated neutral tyrosine radicals in alkaline frozen solution has been determined from isotropic proton and anisotropic (dipolar) ^{13}C- and ^{17}O-hfi with EPR spectroscopy at two frequencies. It is shown that proton hfi spectroscopy only, although sufficient for a global picture, cannot lead to a satisfactory, complete map of the unpaired π-electron spin-density distribution. More information has been obtained from the ^{13}C and ^{17}O isotopes. For example, a ^{13}C-label at C1′ enabled us to determine from the measured dipolar couplings the spin density at this position much more accurately than from the proton hfi at the CH_2 fragment, as it is free from the rotationally disordered orientation of the two methylene β-protons, whereas now also the spin density at the "blind" positions, such as the carbon C4′ and phenol oxygen O4′, could be assessed. Most of the obtained isotropic ^{13}C- and ^{17}O-hfi fit well within the Karplus−Fraenkel theory. Apparently, this relatively simple theory gives a fairly accurate indication of the isotropic ^{13}C- and ^{17}O-hfi of the neutral tyrosine radical. Only the observed isotropic ^{13}C-hfi at C3′ and C5′ do not correspond with the calculated values, which is indicative for a slight in-plane distortion of the aromatic ring structure at these positions. A small rotation of the proton and ^{13}C-hyperfine tensor with respect to the molecular axes system seems to confirm this interpretation. The spin density at C2′ is negative. The relatively large delocalization of the spin density over the carbonyl group of the aromatic ring system of the neutral tyrosine radical indicates that the C4′−O4′ bond has predominant double-bond character.

The characterization of site-selective isotopically labeled neutral tyrosine radicals in vitro forms a solid base for further computational structure optimization of the radical, and for calibrating protein-induced changes in the structure of the neutral tyrosine radical in vivo. Probing the spin density with atomic selectivity at all carbon positions and at the phenol oxygen of radicals of bio-incorporated isotopically labeled tyrosines in vivo, will give unparalleled insight in the interaction between the protein matrix and the tyrosine molecules, such as hydrogen bonding and steric hindrance, which determine the functional properties of the tyrosine moiety in a variety of enzymes. In particular, incorporation of our series of site-selectively labeled tyrosines in Photosystem II of cyanobacteria seems very promising to gain better understanding of the factors determining the functional differences between the symmetry-related so-called Y_D and Y_Z tyrosines (work in progress).

Acknowledgment. We thank Jurgen van Belle for selective deuteration of several tyrosine samples and Dr. N. P. Gritzan and Dr. M. C. van Hemert for their help with some ab initio spin-density calculations. This research was supported by The Netherlands Foundation for Life Sciences (SLW) and Foundation for Chemical Research (SON), both financed by The Netherlands Organization of Scientific Research (NWO).

JA9707872

(90) Johnson, C. R.; Ludwig, M.; Asher, S. A.*J. Am. Chem. Soc.* **1986**, *108*, 905−912.
(91) Beveridge, D. L.; Guth, E. *J. Chem. Phys.* **1971**, *55*, 458−459.
(92) Benson, H. G.; Hudson, A. *Mol. Phys.* **1971**, *20*, 185−187.